

Octacarbonyl Diiron. A Density Functional Study

Heiko Jacobsen[†] and Tom Ziegler*Contribution from the Department of Chemistry, University of Calgary,
2500 University Drive N.W., Calgary, Alberta, Canada T2N 1N4Received October 19, 1995. Revised Manuscript Received March 5, 1996[⊗]

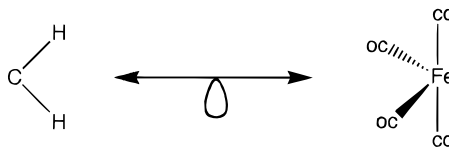
Abstract: The electronic and molecular structures of several isomers of the title compound have been studied by approximate density functional theory. A geometric arrangement with two bridging CO ligands was identified as the most stable structure, similar to that of $\text{Co}_2(\text{CO})_8$. However, the terminal CO ligands in $\text{Fe}_2(\text{CO})_8$ adopt a staggered rather than an eclipsed arrangement. The unbridged isomer is shown to be stabilized by a trans bent distortion. The CO stretching frequencies are reported for the most stable isomers. The theoretical findings are compared to the experimental studies on $\text{Fe}_2(\text{CO})_8$. A mechanism for the isomerization reaction of the dibridged structure to the unbridged structure is proposed.

1. Introduction

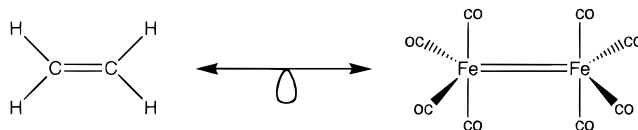
The isolobal analogy¹ relates molecular fragments for which the number, symmetry properties, approximate energy, and shape of the frontier orbitals and the number of electrons are similar. Given this definition, it is possible to transfer various concepts in chemical bonding, which are well-established for the first-row elements, to the chemistry of heavier elements, in particular to the field of transition metal chemistry. Here, the prototypes that are related to hydrocarbon building blocks are transition metal carbonyl fragments. Thus, the $d^8\text{-ML}_4$ species $\text{Fe}(\text{CO})_4$ is isolobal with a methylene unit (Scheme 1). Among the dimers of these fragments are the well-known ethylene molecule and $\text{Fe}_2(\text{CO})_8$, which according to the isolobal analogy can be looked at as an example of a genuine metal–metal double bond (Scheme 2). However, there is no guarantee that the isolobal mapping results in molecules of great thermodynamic or kinetic stability.¹ Isolobal structures might distort into more stable geometries. We mention as an example the higher homologues of ethylene, which possess trans bent rather than planar geometries.² The bonding in these molecules is largely influenced by Pauli repulsion due to the extended electronic core of the heavier group XIV elements.^{3,4a,b}

$\text{Fe}_2(\text{CO})_8$ itself is highly unstable and has so far been observed only in a matrix. In 1971 Poliakoff and Turner⁵ showed that UV/visible photolysis of $\text{Fe}_2(\text{CO})_9$ produced two isomers of $\text{Fe}_2(\text{CO})_8$, namely structures with and without CO ligands in the bridging position. This work constitutes the first application of matrix isolation to a dinuclear carbonyl. In a more recent study, Fletcher, Poliakoff, and Turner⁶ reinvestigated the structure of the $\text{Fe}_2(\text{CO})_8$ molecule, using ^{13}C isotopic methods and photolysis with plane polarized light, together with matrix isolation techniques. For the bridged isomer B- $\text{Fe}_2(\text{CO})_8$ the

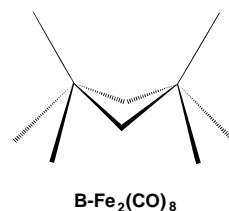
Scheme 1



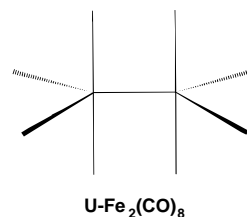
Scheme 2



existence of two bridging CO groups was established. The structure of B- $\text{Fe}_2(\text{CO})_8$ is proposed to be similar to that of $\text{Co}_2(\text{CO})_8$, but with the $\text{M}(\mu\text{-CO})_2\text{M}$ unit closer to planarity.



The results for the unbridged isomer U- $\text{Fe}_2(\text{CO})_8$ are consistent with the D_{2h} Hoffmann structure.



In this paper we present a theoretical study on the title molecule, using approximate density functional theory (DFT), which over the last 15 years has emerged into a powerful tool in studies of organometallic kinetics and energetics.⁷ Our work was prompted for various reasons. First, we hope to support the experimental studies on $\text{Fe}_2(\text{CO})_8$ in the structure determi-

[†] Present address: Anorganisch-Chemisches Institut der Universität Zürich, Winterthurerstrasse 190, CH-8057 Zürich, Switzerland.

[⊗] Abstract published in *Advance ACS Abstracts*, April 1, 1996.

(1) Hoffmann, R. *Angew. Chem., Int. Ed. Engl.* **1982**, *21*, 711.

(2) (a) West, R. *Angew. Chem., Int. Ed. Engl.* **1987**, *26*, 1201. (b) Tsumaraya, T.; Batcheller, S. A.; Masamune, S. *Angew. Chem., Int. Ed. Engl.* **1991**, *30*, 902.

(3) Kutzelnigg, W. *Angew. Chem., Int. Ed. Engl.* **1984**, *23*, 272.

(4) (a) Jacobsen, H.; Ziegler, T. *J. Am. Chem. Soc.* **1994**, *116*, 3667.

(b) Jacobsen, H.; Ziegler, T. *Comments Inorg. Chem.* **1995**, *17*, 301. (c) Jacobsen, H.; Ziegler, T. *Organometallics* **1995**, *14*, 234. (d) Jacobsen, H.; Ziegler, T. *Inorg. Chem.* In press.

(5) Poliakoff, M.; Turner, J. J. *J. Chem. Soc. A* **1971**, 2043.

(6) Fletcher, S. C.; Poliakoff, M.; Turner, J. J. *Inorg. Chem.* **1986**, *25*, 3597.

(7) (a) Ziegler, T. *Pure Appl. Chem.* **1991**, *28*, 1271. (b) Ziegler, T. *Chem. Rev.* **1991**, *91*, 651. (c) Ziegler, T. *Can. J. Chem.* **1995**, *73*, 743.

Table 1. Experimental and Theoretical $\nu(\text{C}-\text{O})$ Stretching Frequencies for $\text{Fe}_2(\text{CO})_9$

	assignment ^d	ν^b	
		expt ^c	theory ^d
a_2''	terminal CO	2064	2058
e'	terminal CO	2037	2032
e'	bridging CO	1847.4	1918

^a According to D_{3h} symmetry. ^b In cm^{-1} . ^c Reference 6, Table I. ^d This work.

nation of this interesting species. Further, the influence of Pauli repulsion on the geometries of $\text{Fe}_2(\text{CO})_8$ will be analyzed. Lastly, we are interested in the nature of the Fe–Fe double bond. This work is part of our investigation of multiple bonding involving heavier main group elements and transition metals.⁴ We will present a concise description of our computational approach before we discuss our findings in more detail.

2. Computational Details

All calculations are based on approximate density functional theory. Frequency calculations were based on the local density approximation (LDA) in the parametrization of Vosko, Wilk, and Nussair.⁸ The other calculations were performed on the nonlocal level of theory (NL-SCF), where gradient corrections due to Becke⁹ and Perdew¹⁰ were added self-consistently. The calculations were performed using the Amsterdam Density Functional package ADF,¹¹ release 1.1.3. Use was made of the frozen core approximation. For C and O, the valence shells were described using a double- ζ STO basis, augmented by one d -STO polarization function (ADF database III). For the ns , np , nd , $(n+1)s$, and $(n+1)p$ shells on Fe, a triple- ζ STO basis was employed (ADF database IV, augmented by $\alpha_{4p} = 0.90, 1.40, \text{ and } 2.30$). The numerical integration grid was chosen in a way that significant test integrals are evaluated with an accuracy of at least four significant digits. In the geometry optimization, the absolute values of the final gradients were in general smaller than 0.001 au. Frequencies were evaluated by finite difference, using a one point displacement formula. Due to numerical noise, all frequencies with an absolute value less than 100 wavenumbers are considered insignificant, and are neglected in the analysis.

3. Results and Discussion

The Parent Molecule $\text{Fe}_2(\text{CO})_9$. To judge the performance of our method, calculations were done on the well-known molecule enneacarbonyliron. In structure **1**, we compare our optimized NL-SCF geometry with the crystal structure¹² of $\text{Fe}_2(\text{CO})_9$. The agreement between theory and experiment is excellent, with a maximum deviation of 1.1 pm for bond lengths and 0.1° for bond angles. Values for the $\nu(\text{C}-\text{O})$ stretching frequencies are presented in Table 1. For ligands in the terminal position, the experimental frequencies are astonishingly well reproduced. For a bridging CO ligand, we observe that the value for $\nu(\text{C}-\text{O})$ is overestimated by about 4%. In general, these results indicate that DFT should also be capable of producing reliable geometries and good frequencies for the various isomers of $\text{Fe}_2(\text{CO})_8$.

The Bridged Isomer $\text{B-Fe}_2(\text{CO})_8$. Two possible reaction channels lead from $\text{Fe}_2(\text{CO})_9$ to $\text{B-Fe}_2(\text{CO})_8$, namely the dissociation of a terminal t -CO or of a bridging μ -CO ligand. We calculated the energies needed to abstract one of these

Table 2. Experimental and Theoretical $\nu(\text{C}-\text{O})$ Stretching Frequencies^a and Absorption Intensities^b for $\text{B-Fe}_2(\text{CO})_8$

	bridging CO			terminal CO		
	experi- ment ^c	theory ^d		experi- ment ^c	theory ^d	
		2a (C_s)	2b (C_{2v})		2a (C_s)	2b (C_{2v})
1857 (ww)	1880 (57)	1890 (168)	2055 (ss)	2095 (48)	2086 (2)	
1814 (b)	1860 (725)	1870 (679)	2032 (m)	2052 (1600)	2048 (1458)	
			2022 (s)	2031 (834)	2020 (1426)	
				2022 (1274)	2012 (1332)	
				2018 (460)	2007 (189)	
				2014 (328)	2006 (0)	

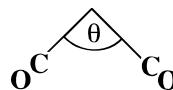
^a In cm^{-1} . ^b In km/mol . Intensities in parentheses. ^c Reference 6, Table I. Intensity assignments are estimated according to the reported spectrum. ^d This work.

ligands to be $\text{BE}(t\text{-CO}) = 171 \text{ kJ/mol}$ and $\text{BE}(\mu\text{-CO}) = 195 \text{ kJ/mol}$. Thus, the removal of the terminal ligand is energetically favored by 24 kJ/mol. Photolysis experiments with polarized light also provide evidence that the primary photochemical step is the loss of a terminal CO group.⁶ One should expect that this step leads to a tribridged $\text{Fe}_2(\text{CO})_8$ isomer of C_s symmetry. However, our geometry optimization indicates that one of the μ -CO ligands bends away out of the bridging position, resulting in the dibridged structure **2a**. The Fe–Fe separation in this molecule amounts to 250.6 pm, being about 2 pm shorter than in $\text{Fe}_2(\text{CO})_9$. The distances between the formerly μ -CO ligand and the two metal centers are 283.0 and 175.7 pm. Although only loosely bound to one of the Fe centers, this ligand is still bent toward the bridging region of **2a**, so that the free coordination site for this complex is a terminal rather than a bridging position.

The dissociation of a bridging ligand of $\text{Fe}_2(\text{CO})_9$ leads to the C_{2v} structure **2b**. The Fe–Fe distance in this molecule is 246.7 pm, clearly shorter than in $\text{Fe}_2(\text{CO})_9$ or **2a**. We found that **2b** is 6 kJ/mol higher in energy than **2a**. This structure can be viewed as a rotomer of **2a** where now the terminal CO ligands on the two Fe centers take on an eclipsed configuration. The vacant coordination site for this structure is clearly a bridging position.

Observed and calculated IR spectra for $\text{B-Fe}_2(\text{CO})_8$ are reported in Table 2. Comparing the stretching frequencies for the bridging CO ligands, we find that the calculated values for structures **2a** and **2b** are in reasonable agreement with the experiment, with a somewhat better match for structure **2a**. As expected, the DFT calculation overestimates the stretching frequency for the bridging CO ligands by about 1–3%. The notion that the observed $\nu(\text{C}-\text{O})$ stretching frequencies are in favor of isomer **2a** is strongly supported when the intensity pattern for the terminal CO stretches is analyzed. For the C_{2v} isomer **2b**, the three t - $\nu(\text{C}-\text{O})$ frequencies should appear with comparable intensities. On the other hand, the C_s structure would give rise to one significantly weaker band. The calculated intensity pattern strong–medium–strong matches well the one observed for $\text{B-Fe}_2(\text{CO})_8$.

Under the assumption that the terminal and bridging stretches do not couple, the intensities of the symmetric and asymmetric stretch of the bridging CO ligands allows an estimate^{6,13} of the angle θ between these groups:



The estimated value amounts to $\theta = 140^\circ \pm 5^\circ$. The optimized

- (8) Vosko, S. J.; Wilk, M.; Nussair, M. *Can. J. Phys.* **1980**, *58*, 1200.
 (9) (a) Becke, A. *J. Chem. Phys.* **1986**, *84*, 4524. (b) Becke, A. *J. Chem. Phys.* **1988**, *88*, 1053. (c) Becke, A. *Phys. Rev.* **1988**, *A38*, 3098.
 (10) (a) Perdew, J. P. *Phys. Rev.* **1986**, *B33*, 8822. (b) Perdew, J. P. *Phys. Rev.* **1986**, *B34*, 7406.
 (11) (a) Baerends, E. J.; Ellis, D. E.; Ros, P. E. *Chem. Phys.* **1973**, *2*, 41. (b) teVelde, G.; Baerends, E. J. *J. Comp. Phys.* **1992**, *99*, 84.
 (12) Cotton, F. A.; Troup, J. M. *J. Chem. Soc. A* **1974**, 800.
 (13) Lukehart, C. M. *Fundamental Transition Metal Organometallic Chemistry*; Brooks/Cole: Monterey, CA, 1985; p 78.

geometries for $\text{B-Fe}_2(\text{CO})_8$ give angles $\theta = 140^\circ$ for **2a** and $\theta = 145^\circ$ for **2b**. Thus, this structural parameter is well-represented by both of the dibridged structures, again with a slightly better agreement for the C_s isomer.

We conclude our discussion of the $\text{B-Fe}_2(\text{CO})_8$ with its possible thermal reactions.⁶ Under annealing, $\text{B-Fe}_2(\text{CO})_8$ can either isomerize to the unbridged form, recombine with CO to form $\text{Fe}_2(\text{CO})_9$, or react with other dopant in the matrix. When the matrix is doped with ^{13}CO or N_2 , it is observed that both $\text{Fe}_2(\text{CO})_8(^{13}\text{CO})$, with ^{13}CO in a terminal position, and $\text{Fe}_2(\text{CO})_8(\text{N}_2)$, with N_2 in a terminal position, are formed.⁶ These observations can be most easily rationalized with **2a** as the reactive species, possessing a vacant terminal rather than a vacant bridging position. For **2b**, Fletcher and co-workers⁶ suggest a reaction pathway which involves singly bridged $\text{Fe}_2(\text{CO})_8$ as a transient species. The vacant bridging position is now turned into a vacant terminal position. This molecule now can recombine with CO or N_2 , or can further transform into $\text{U-Fe}_2(\text{CO})_8$.

The Unbridged Isomer U-Fe₂(CO)₈. The starting point for our analysis of $\text{U-Fe}_2(\text{CO})_8$ is the D_{2h} Hoffmann structure. Its optimized geometry is displayed in **3a**. Compared to the doubly bridged species **2a**, the unbridged **3a** is 111 kJ/mol higher in energy. An interesting structural parameter is the Fe–Fe separation, $d_{\text{Fe-Fe}} = 267.1$ pm, which is significantly longer than that for the doubly bridged systems.

In order to analyze the Fe–Fe double bond, we consider the bond forming reaction in which two triplet $\text{Fe}(\text{CO})_4$ fragments combine to $\text{U-Fe}_2(\text{CO})_8$. This process is associated with the so-called bond snapping energy, which can be decomposed¹⁴ into two main components, namely the steric interaction term ΔE^0 and the electronic interaction term ΔE_{int} :

$$\text{BE}_{\text{snap}} = -[\Delta E^0 + \Delta E_{\text{int}}] \quad (1)$$

ΔE^0 is in most cases dominated by the contribution from the so-called Pauli repulsion, which is directly related to the two-orbital three- or four-electron interactions between occupied orbitals on both fragments. Whereas ΔE^0 is mostly destabilizing in nature, the term ΔE_{int} introduces the attractive orbital interactions between occupied and virtual orbitals on the two fragments. We further can decompose our electronic interaction energy due to different symmetry contributions:

$$\Delta E_{\text{int}} = \sum_{\Gamma} \Delta E_{\text{int}}^{\Gamma} \quad (2)$$

The different $\Delta E_{\text{int}}^{\Gamma}$ terms can then be classified according to σ and π interactions. For $\text{U-Fe}_2(\text{CO})_8$ we find $\Delta E^0 = 85$ kJ/mol and $\Delta E_{\text{int}} = -291$ kJ/mol, resulting in a value for the bond snapping energy, BE_{snap} , of 206 kJ/mol. However, the electronic term is dominated by the σ interaction, $\Delta E_{\text{int},\sigma} = 245$ kJ/mol, whereas the π component is rather weak, $\Delta E_{\text{int},\pi} = 46$ kJ/mol. For **3a**, the σ/π ratio amounts to 5.32, which was roughly twice as much as the value obtained for ethylene,^{4a} $\sigma/\pi = 2.78$. This indicates that for a $\text{Fe}_2(\text{CO})_8$ a true σ/π double bond might not be favorable on electronic grounds.

Further insight into the Fe–Fe bond in **3a** is gained when the frontier orbitals are analyzed. Figure 1 displays the two highest occupied and the two lowest unoccupied orbitals for $\text{U-Fe}_2(\text{CO})_8$. The σ (a_g) and the π (b_{3u}) orbitals are very close in energy, with the σ orbital being the HOMO. This resembles

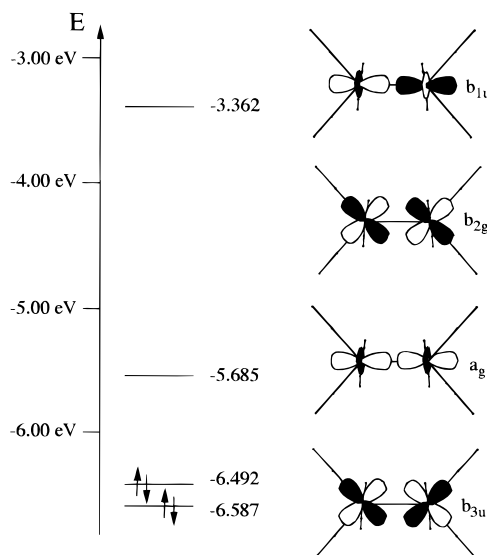
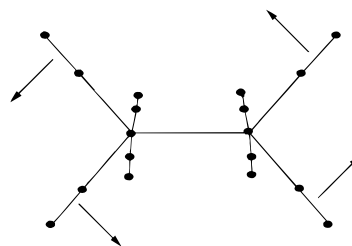


Figure 1. Frontier orbital diagram for **3a**, the Hoffmann structure of $\text{Fe}_2(\text{CO})_8$.

the fact that $\text{Fe}(\text{CO})_4$ has a small singlet–triplet splitting¹⁵ ($\Delta E_{\text{ST}} = -7$ kJ/mol), with the a_g σ -type orbital as HOMO. It is further remarkable that the σ/π^* splitting (HOMO–LUMO gap) only amounts to 0.95 eV. Even the π and σ^* orbitals are separated by only 3.22 eV.

The trans bent structure of the heavier ethylene analogues can be explained in terms of a second-order Jahn–Teller distortion.^{4a} The π bonding and the σ^* antibonding orbitals come close in energy (for Si_2H_4 $\Delta E = 4.5$ eV) so that a geometry distortion allowing these orbitals to mix leads to an overall stabilization of the molecule. This suggests that for **3a** a Jahn–Teller distortion might be possible, with a distortion mode that would allow the a_g (HOMO) and b_{2g} (LUMO) to interact. The corresponding normal mode should then be of b_{2g} symmetry, and reduces the symmetry of the molecule from D_{2h} to C_{2h} .



The optimized trans-bent geometry for $\text{U-Fe}_2(\text{CO})_8$ is shown in **3b**. We find that **3b** is 81 kJ/mol more stable in energy than **3a**. Although two of the former equatorial CO ligands move toward a bridging position, the two Fe–C bond lengths are quite different. Thus, this structure still has to be considered an unbridged rather than a dibridged arrangement. Of further interest is the fact that the Fe–Fe bond shortens under the trans-bent distortion, indicating a stabilization of the Fe–Fe bond.

In Figure 2, 2D contour plots of the frontier orbitals of **3a** (2a–2d) together with the corresponding orbitals of **3b** (2e–2h) are depicted. The plane shown contains the Fe–Fe bond as well as the axial and trans-bent CO ligands. Only the region around the Fe–Fe bond is shown. The a_g and the b_{2g} orbitals in D_{2h} symmetry correlate with the two a_g orbitals in C_{2h} , whereas the counterparts of the b_{1u} and b_{3u} orbitals in D_{2h} symmetry are the b_u orbitals of C_{2h} . Under trans-bending, the

(14) (a) Baerends, E. J.; Roozendaal, A. *NATO ASI* **1986**, C176, 159. (b) Ziegler, T. *NATO ASI* **1991**, C378, 367.

(15) Li, J.; Schreckenbach, G.; Ziegler, T. *J. Am. Chem. Soc.* **1995**, *117*, 486.

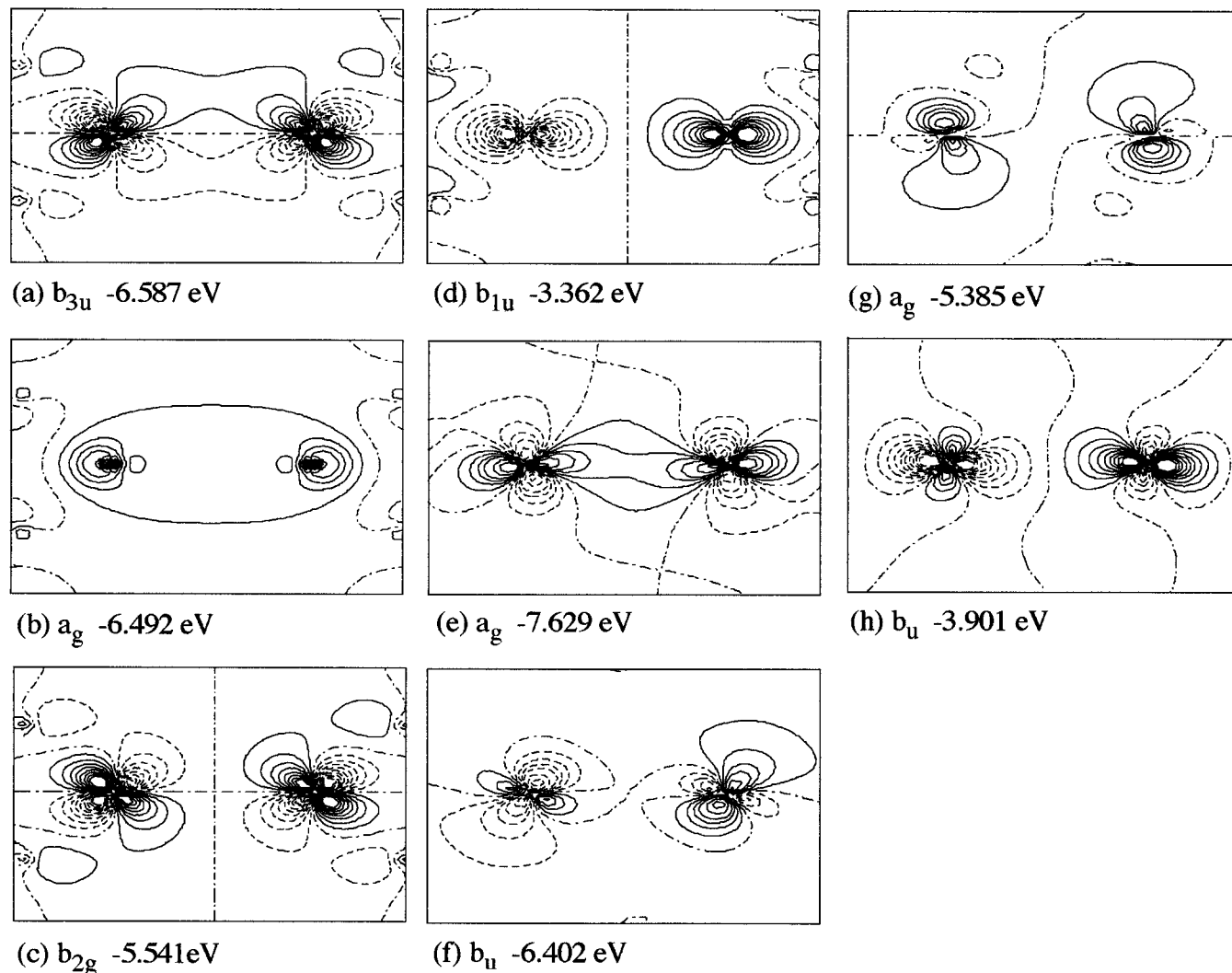


Figure 2. 2D contour plots for the frontier orbitals of the double bonded structure **3a** (a–d), as well as for the corresponding orbitals of the trans-bent isomer **3b**. Contour values chosen are 0, ± 0.05 , ± 0.10 , ± 0.15 , ± 0.20 , ± 0.30 , and ± 0.40 au. Positive values are represented by solid lines, negative values are represented by dashed lines. The zero value is indicated by a dash-dotted line.

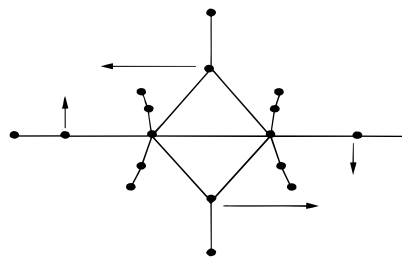
a_g orbital is clearly stabilized: $a_g(D_{2h}) -6.492$ eV \rightarrow $a_g(C_{2h}) -7.629$ eV. Since under this distortion the $\pi(b_{3u})$ and the $\sigma^*(b_{1u})$ orbital do also mix, one would expect an additional stabilization of the b_{3u} orbital. However, the b_{3u} orbital energy increases slightly: $b_{3u}(D_{2h}) -6.587$ eV \rightarrow $b_u(C_{2h}) -6.402$ eV. For **3b**, the π -bonding orbital now becomes the HOMO. This can be rationalized by further interaction of the migrating CO ligands with the Fe centers.

We now turn to the IR spectrum of $U-Fe_2(CO)_8$. The experimental and calculated $\nu(C-O)$ stretching frequencies are collected in Table 3. For both the **3a** and the **3b** geometries the calculated frequencies are in fair agreement with the experiment. The observed pattern of the absorption intensities is in accord with that for structure **3b**. The IR dichroism spectrum is compatible with both D_{2h} as well as C_{2h} geometries.

Structural Alternatives. For both the isomers of octacarbonyldiiron, namely for $U-Fe_2(CO)_8$ as well as for $B-Fe_2(CO)_8$, one can think of alternative geometries. For the unbridged structure, one might consider a D_{3d} structure such as the one observed¹⁶ for $Co_2(CO)_8$. The optimized geometry for the iron analogue is displayed in **4**. This molecule possesses a triplet ground state. An interesting structural parameter is the short Fe–Fe distance of 252.2 pm. We calculated **4** to be 5 kJ/mol

more stable than the Hoffmann structure **3a**. However, the IR spectrum of $U-Fe_2(CO)_8$ excludes isomer **4**, since in D_{3d} symmetry only three rather than four $\nu(C-O)$ stretching frequencies are expected.

When discussing trans bending of $U-Fe_2(CO)_8$, one might consider a distortion which leads to a symmetrical structure. The resulting geometry is the D_{2h} structure **5**, a variation of $B-Fe_2(CO)_8$. The Fe–Fe bond length for this isomer is 255.5 pm, about 5 pm longer than for the C_s structure **2a**. Our frequency analysis reveals that this structure corresponds to a transition state on the energy hyper surface of $Fe_2(CO)_8$. The normal mode corresponding to the imaginary frequency of 267 cm^{-1} would lead **5** into the trans-bent geometry **3b**.



To analyze trends in bonding of the bridged molecules, we might perform a bond analysis in which we react a suitably prepared

(16) (a) Noack, K. *Helv. Chim. Acta* **1964**, *47*, 1064. (b) Noack, K. *Helv. Chim. Acta* **1964**, *47*, 1555.

Table 3. Experimental and Theoretical $\nu(\text{C}-\text{O})$ Stretching Frequencies^a and Absorption Intensities^b for U-Fe₂(CO)₈

experiment ^c	theory ^d	
	3b (<i>C</i> _{2h})	3a (<i>D</i> _{2h})
1974 (w)	1951 (211)	2000 (1555)
1978 (w)	1995 (613)	2007 (254)
2006 (ss)	2032 (2034)	2036 (1951)
2038 (s)	2036 (1484)	2039 (1692)

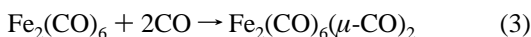
^a In cm⁻¹. ^b In km/mol. Intensities in parentheses. ^c Reference 6, Table I. Intensity assignments are estimated according to the reported spectrum. ^d This work.

Table 4. Analysis of Bonding between the Two Bridging CO Ligands and the Fe₂(CO)₆ Fragments for Various Fe₂(CO)₈ Isomers^a

	ΔE^0	ΔE_{int}	BE	$E_{\text{prep}}^{\text{rel}}$
2a (<i>C</i> _s)	1051	-1543	492	0
2b (<i>C</i> _{2v})	1099	-1591	492	6
5 (<i>D</i> _{2h})	1172	-1659	487	58
3b (<i>C</i> _{2h})	817	-1338	521	58

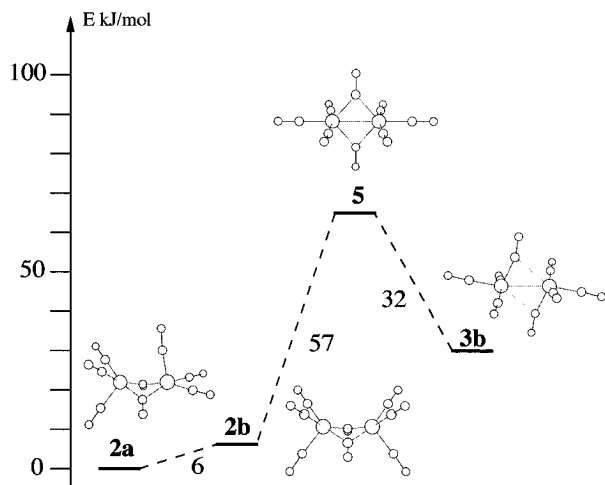
^a Energies in kJ/mol.

Fe₂(CO)₆ fragment with two CO ligands:



The bond snapping energy associated with this process again is broken down into steric and electronic contributions, eq 1. We further include the energy which is required to promote the (CO)₂ and Fe₂(CO)₆ fragments into the respective orientations of the final molecules. To this end the sum of the fragment energies of **2a** is set to zero, and the energies of the fragments of the remaining structures are taken relative to **2a**. We call this energy the relative preparation energy, $E_{\text{prep}}^{\text{rel}}$. The results of this analysis are presented in Table 4. If we compare the two dibridged structures **2a** and **2b**, it turns out that they have identical bonding energies. **2a** has a somewhat stronger orbital interaction, but shows also a larger steric repulsion. The energy difference between this two structures arises from the different preparation energies. The symmetrical bridged structure has a strongly enhanced orbital interaction. However, this cannot compensate for the increased steric repulsion so that as a net result **5** has a lower bond energy than the isomers of **2**. It is the balance between ΔE^0 and ΔE_{int} plus the differences in $E_{\text{prep}}^{\text{rel}}$ which favors structure **2** over **5**. For the sake of comparison, we also included an analysis for the trans-bent geometry **3b**. This molecule exhibits the largest value for BE. However, due to a high preparation energy, **3b** is higher in energy than structures **2**.

Isomerization Reaction B-Fe₂(CO)₈ → U-Fe₂(CO)₈. We shall conclude our discussion commenting on how dibridged Fe₂(CO)₈ might transform into the unbridged form. Under annealing, **2a** might either recombine with CO or rotate into the isomer **2b**. Opening the angle between the two bridging

**Figure 3.** A proposed reaction mechanism for the isomerization reaction B-Fe₂(CO)₈ → U-Fe₂(CO)₈.

CO groups from 145° to 180°, the transition state **5** is reached. This structure then relaxes to give the trans-bent isomer **3b**. A schematic profile for this process is outlined in Figure 3.

4. Conclusion

We have investigated the structure and energetics of several isomers of Fe₂(CO)₈. The following stability ranking can be obtained: **2a**, *C*_s (0 kJ/mol) > **2b**, *C*_{2v} (6 kJ/mol) > **3b**, *C*_{2v} (29 kJ/mol) > **4** (105 kJ/mol) > **3a** (110 kJ/mol). Here, the energy of the most stable isomer, the *C*_s structure **2a**, is set to zero, and the other systems are higher in energy by the amount reported in parentheses. As predicted in the experiment, we found a doubly bridged structure to be the most stable arrangement for octacarbonyldiiron. However, we predict the terminal CO groups on the two Fe centers to adopt a staggered rather than an eclipsed conformation. We found that the unsupported Fe-Fe double bond has only a weak π component. Thus, the unbridged structure is stabilized by a trans-bent distortion.

Acknowledgment. The work presented here was supported by the Natural Sciences and Engineering Research Council of Canada (NSERC) and by the donors of the Petroleum Research Fund, administered by the American Chemical Society (ACS-PRF No. 27023-AC3). H.J. acknowledges a scholarship from the chemistry department at the University of Calgary.

Supporting Information Available: Structures as well as bond distance and angle data for **1**, **2a**, **2b**, **3a**, **3b**, **4**, and **5** (7 pages). This material is contained in many libraries on microfiche, immediately follows this article in the microfilm version of the journal, can be ordered from the ACS, and can be downloaded from the Internet; see any current masthead page for ordering information and Internet access instructions.

JA953509G